Journal of Quantitative Spectroscopy & Radiative Transfer 220 (2018) 106–113

Contents lists available at ScienceDirect

Journal of Quantitative Spectroscopy & Radiative Transfer

journal homepage: www.elsevier.com/locate/jqsrt

The $4d^8nf$ (n = 5 and 6) and $4d^87p$ configurations in the spectrum of four times ionized indium (In V)

A.N. Ryabtsev

Russian Academy of Sciences, Institute of Spectroscopy, Troitsk, Moscow 108840, Russia

ARTICLE INFO

Article history:
Received 4 September 2018
Revised 13 September 2018
Accepted 13 September 2018
Available online 13 September 2018

Keywords:
Atomic ion spectra
Wavelengths
Energy levels
Transition probabilities
Parametric calculations

ABSTRACT

The spectrum of the In^{+4} ion was studied in the region below 222 Å. The $4d^9$ – ($4d^8nf$ ($n > 4$) + $4d^8np$ ($n > 6$)) transitions were analyzed. 74 spectral lines of the transitions from the levels of the $4d^85f$, $4d^86f$ and $4d^87p$ configurations were identified. Previous analysis of the $4d^9 - 4d^8$ (5f + 7p) transitions was revised.

1. Introduction

Four times ionized indium has a ground state configuration $4d^9$. In a comparison with previous works [1–5] the analysis of its spectrum was recently extended [6]. In particular, 19 new lines in the region 204–219 Å were identified as the $4d^9$ – ($4d^85f + 4d^87p$) transitions. It was noticed at our analysis of the In^{5+} spectrum [7] that there are substantially more lines of In V in this region, which could belong to these transitions. Thus the analysis of In V could be further extended.

On the other hand, as was found recently by Kramida [8] the Cowan code [9] contains an error in calculations of Rydberg configurations. In application to In V, this error affects the values of the configuration interaction (CI) integrals within the $4d^8nf$ series. An addition of the $4d^74f5s$ configuration to the set of the odd configurations results in appearance of non zero $R_d{}^0$(4d4f,4dnf) (n > 4) CI integrals that is prohibited by Brillouin's theorem [9]. Their presence leads to large shifts of the calculated level positions and may influence the identification of In V made in [6].

In this work the previous analysis [6] of the $4d^9$ – ($4d^85f + 4d^87p$) transitions was revised and extended and 17 lines of the $4d^9$–$4d^86f$ transitions were identified.

2. Experimental details

The spectra of indium for this study were obtained previously [5,7]. Briefly, the spectra were excited in a vacuum spark and recorded on a 3-m grazing incidence spectrograph equipped with a 3600 lines/mm holographic grating. Old spectra [5] were obtained on SWR type photographic plates. FUJI Imaging Plate BAS-TR2025 was used for recording of new spectra in [7]. Wavelength measurements were made on the photographic plates with estimated uncertainty ±0.005 Å for the unperturbed lines. The spectra obtained on the imaging plate were used for intensity measurements and observations of line intensities at different excitation conditions in the spark.

A part of the indium spectrum in the region 203.7–207.7 Å obtained at two different conditions of excitation is presented in Fig. 1. The In V and In VI lines identified in this work and in [7] are marked. The different behavior of the In V and In VI line intensities in a comparison of “cold” and “hot” spectra is clearly seen. Henceforth in this paper, the behavior of the line intensity at different excitation conditions is called "an ionization character" of the line.

As in [7] the intensities were measured without taking into account the wavelength dependence of the spectrograph efficiencies and imaging plate sensitivity. The intensity I = 400 was attributed to the strongest identified line $4d^9\ {}^2D_{5/2} - 4d^85f(1G)^2F_{7/2}$ (204.985 Å). The $4d^9\ {}^2D_{5/2} - 4d^84f({}^1S)^2F_{7/2}$ line at 223.995 Å has intensity 500 in this scale.

3. Results and discussion

Configuration interaction calculations with the Cowan codes [9] modified by Kramida [10] were performed for the set of the configurations close to the one in previous analyses of In V [6]. The set consists of the $4d^9$ + ($4d^8ns$ (n = 5,6) + $4d^8nd$

E-mail address: ryabtsev@isan.troitsk.ru

https://doi.org/10.1016/j.jqsrt.2018.09.011
0022-4073/

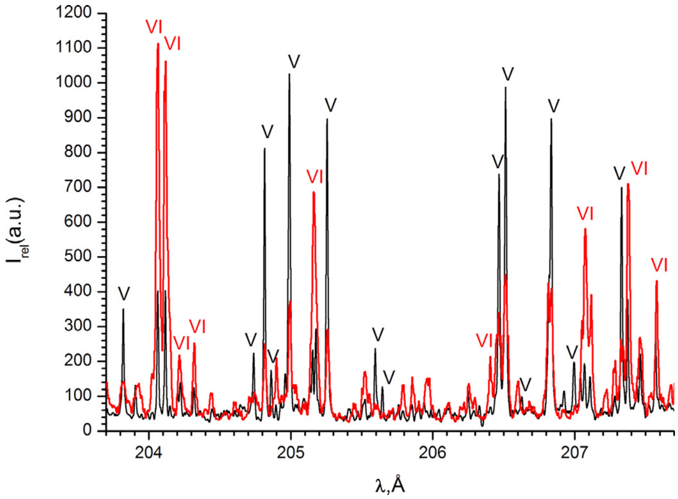

Fig. 1. Indium spectrum in the 203.7–207.7 Å region excited in two modes of a vacuum spark operation: "cold" –black, "hot" – gray (red on the Web only). Relative intensity of the lines is given in arbitrary units. Lines of In V identified in this work and In VI lines from [7] are marked respectively by V and VI.

$(n=5,6)+4d^75s^2$) even configurations and $4d^8np$ $(n=5–8)+4d^8nf$ $(n=4–8)+4p^54d^{10}+4d^75s5p+4d^74f5s$ odd configurations. In the first approximation *ab initio* values of the energy parameters were modified by the same scaling factors as in [6]. Such predicted energy levels and transition probabilities were used for a start of the spectrum identification with the aid of the program IDEN2 [11]. Least-squares fitting of the calculated to found levels was used in an iterative procedure for the final identification of the spectrum. The identified In V lines, the energy levels and final energy parameters are presented respectively in Tables 1–3.

The list of identified transitions contains 74 lines in the region 192–222 Å including 57 lines of the $4d^9-(4d^85f+4d^87p)$ transitions and 17 lines of the $4d^9$ – $4d^86f$ transitions. 50 and 14 levels were found respectively in the $4d^85f+4d^87p$ and $4d^86f$ configurations. The level energy errors due to uncertainties in the wavelength measurements are estimated to be from 8 to 13 cm^{-1} depending on the corresponding wavelengths and a number of lines from a particular level.

The interaction of the Rydberg configurations with the unknown $4d^75s5p$ configuration was the main difficulty in the interpretation of the In V spectrum in this region. The estimated level spread of the $4d^75s5p$ configuration is from 405,000 through

Table 1
Identified lines of the $4d^9-(4d^85f+4d^87p+4d^86f)$ transitions in In V.

I[a]	gA[b], (10^8c^{-1})	λ(Å)[c]	o.-c.[d]	ν(cm^{-1})	Lower level	Upper level	
						Term.	E(cm^{-1})
60	299	192.080		520617.5	$^2D_{5/2}$	$4d^86f(^3P)^2G_{7/2}$	520,617
70	466	192.205		520277.3	$^2D_{3/2}$	$4d^86f(1\,G)^2D_{3/2}$	527,449
115	642	192.590		519238.8	$^2D_{3/2}$	$4d^86f(1\,G)^2D_{5/2}$	526,411
60	94	193.481		516845.5	$^2D_{3/2}$	$4d^86f(1\,G)^2F_{5/2}$	524,017
60	87	194.115		515157.5	$^2D_{5/2}$	$4d^85f(^1S)^2F_{7/2}$	515,158
120	454	194.414		514365.2	$^2D_{5/2}$	$4d^86f(^3P)^2F_{5/2}$	514,365
180	23	195.172		512368.6	$^2D_{3/2}$	$4d^86f(^3P)^4G_{5/2}$	519,540
230	1118	195.876	−0.001	510528.1	$^2D_{5/2}$	$4d^86f(^3F)^2D_{5/2}$	510,526
230	1083	196.297		509431.4	$^2D_{5/2}$	$4d^86f(^3F)^2F_{7/2}$	509,431
150	163	196.631	0.000	508566.5	$^2D_{5/2}$	$4d^86f(^3F)^2D_{3/2}$	508,566
95	127	197.119		507309.1	$^2D_{3/2}$	$4d^86f(^3P)^4D_{3/2}$	514,481
180	428	197.156	0.000	507211.5	$^2D_{5/2}$	$4d^86f(^3F)^2F_{5/2}$	507,212
75	100	197.699		505819.7	$^2D_{5/2}$	$4d^86f(^3F)^4G_{7/2}$	505,820
100	186	198.668	0.001	503351.6	$^2D_{3/2}$	$4d^86f(^3F)^2D_{5/2}$	510,526
200	548	199.327		501687.2	$^2D_{5/2}$	$4d^86f(^3F)^4P_{5/2}$	501,688
180	564	199.444	0.000	501394.4	$^2D_{3/2}$	$4d^86f(^3F)^2D_{3/2}$	508,566
220	334	199.704		500740.6	$^2D_{5/2}$	$4d^86f(^3F)^2F_{7/2}$	500,741
140	414	199.984	0.000	500040.8	$^2D_{3/2}$	$4d^86f(^3F)^2F_{5/2}$	507,212
80	86	203.321		491831.9	$^2D_{3/2}$	$4d^87p(1\,G)^2F_{5/2}$	499,004
130	178	203.815	0.003	490640.1	$^2D_{5/2}$	$4d^85f(1\,G)^2D_{3/2}$	490,648
70	49	204.735		488437.0	$^2D_{3/2}$	$4d^87p(^1D)^2D_{3/2}$	495,609
310	54	204.811 ST		488255.7	$^2D_{5/2}$	$4d^87p(^3P)^4D_{7/2}$	488,256
60	30	204.858		488143.7	$^2D_{5/2}$	$4d^87p(^3P)^4P_{5/2}$	488,144
400	3369	204.985		487839.9	$^2D_{5/2}$	$4d^85f(1\,G)^2F_{7/2}$	487,840
340	2208	205.252 ST		487206.4	$^2D_{5/2}$	$4d^85f(1\,G)^2D_{5/2}$	487,206
85	97	205.591		486402.9	$^2D_{5/2}$	$4d^87p(^3P)^4D_{5/2}$	486,403
50	75	205.641		486283.6	$^2D_{5/2}$	$4d^85f(1\,G)^2G_{7/2}$	486,284
280	410	206.464 ST		484345.7	$^2D_{3/2}$	$4d^85f(^3P)^2F_{5/2}$	491,517
380	3728	206.510		484237.3	$^2D_{3/2}$	$4d^85f(^3P)^2F_{5/2}$	491,409
30	27	206.623	0.003	483973.0	$^2D_{5/2}$	$4d^85f(1\,G)^2F_{5/2}$	483,979
330	1560	206.831 ST	−0.004	483486.0	$^2D_{3/2}$	$4d^85f(1\,G)^2D_{3/2}$	490,648
70	128	206.992		483110.7	$^2D_{5/2}$	$4d^85f(^1D)^2D_{5/2}$	483,111
270	692	207.326 ST		482333.1	$^2D_{5/2}$	$4d^85f(1\,G)^2F_{7/2}$	482,333
50	171	207.794		481246.5	$^2D_{3/2}$	$4d^85f(1\,G)^2D_{3/2}$	488,418
40	25	208.392		479864.6	$^2D_{5/2}$	$4d^85f(^3P)^4D_{7/2}$	479,865
100	141	208.714		479125.7	$^2D_{5/2}$	$4d^85f(^3P)^4G_{7/2}$	479,126
60	30	209.090		478262.5	$^2D_{5/2}$	$4d^85f(^3P)^4D_{5/2}$	478,262
210	120	209.293		477798.8	$^2D_{5/2}$	$4d^87p(^3F)^4G_{7/2}$	477,799
80	51	209.598 ST		477103.1	$^2D_{3/2}$	$4d^85f(1\,G)^2D_{3/2}$	484,275
65	59	209.725	−0.003	476814.9	$^2D_{3/2}$	$4d^85f(1\,G)^2F_{5/2}$	483,979
360	990	209.781 ST		476686.7	$^2D_{5/2}$	$4d^85f(^3P)^2G_{7/2}$	476,687
170	243	210.257		475607.3	$^2D_{3/2}$	$4d^85f(1\,G)^2P_{1/2}$	482,779
310	565	210.637		474749.7	$^2D_{5/2}$	$4d^85f(^3P)^2F_{5/2}$	474,750
135	38	210.709		474587.7	$^2D_{3/2}$	$4d^85f(^1D)^2P_{1/2}$	481,759

(*continued on next page*)